

Semantics Alignment via Split Learning for Resilient Multi-User Semantic Communication

Jinhyuk Choi, [†]Jihong Park, [‡]Seung-Woo Ko, [†]Jinho Choi, *Mehdi Bennis, and Seong-Lyun Kim

Abstract—Recent studies on semantic communication commonly rely on neural network (NN) based transceivers such as deep joint source and channel coding (DeepJSCC). Unlike traditional transceivers, these neural transceivers are trainable using actual source data and channels, enabling them to extract and communicate semantics. On the flip side, each neural transceiver is inherently biased towards specific source data and channels, making different transceivers difficult to understand intended semantics, particularly upon their initial encounter. To align semantics over multiple neural transceivers, we propose a distributed learning based solution, which leverages split learning (SL) and partial NN fine-tuning techniques. In this method, referred to as SL with layer freezing (SLF), each encoder downloads a misaligned decoder, and locally fine-tunes a fraction of these encoder-decoder NN layers. By adjusting this fraction, SLF controls computing and communication costs. Simulation results confirm the effectiveness of SLF in aligning semantics under different source data and channel dissimilarities, in terms of classification accuracy, reconstruction errors, and recovery time for comprehending intended semantics from misalignment.

Index Terms—DeepJSCC, neural transceiver, split learning, fine-tuning, semantic communication.

I. INTRODUCTION

A. Semantic Communication using Neural Transceivers

While recent advances in machine learning have transformed communication system’s design principles [1], it can be argued that semantic communication (SC) is an area that significantly benefits from the application of machine learning techniques [2]–[4]. While classical communication focuses on transferring the bit representations of data over noisy channels to reconstruct the original data [5], SC aims to convey meaningful or *semantic representations (SRs)* of the data, tailored for specific tasks such as classification, control, and other tasks [2]–[4]. To enable SC built upon classical communication operations, one promising approach is via artificial intelligence (AI) native transceiver designs that utilize a neural network (NN) as a trainable end-to-end transceiver, as elaborated next.

An NN is ideally a universal function approximator [6], and has a great potential in simultaneously emulating multiple functionalities that are tantamount to a composite function.

J. Choi and S.-L. Kim are with the School of Electrical and Electronic Engineering, Yonsei University, Seoul 03722, Korea.

[†]J. Park and J. Choi are with the School of Information Technology, Deakin University, Geelong, VIC 3220, Australia.

[‡]S.-W. Ko is with the Department of Smart Mobility Engineering, Inha University, Incheon 21999, Korea.

*M. Bennis is with the Centre for Wireless Communications, University of Oulu, Oulu 90014, Finland.

J. Park, S.-W. Ko, and S.-L. Kim are corresponding authors (email: jihong.park@deakin.edu.au, swko@inha.ac.kr, slkim@yonsei.ac.kr).

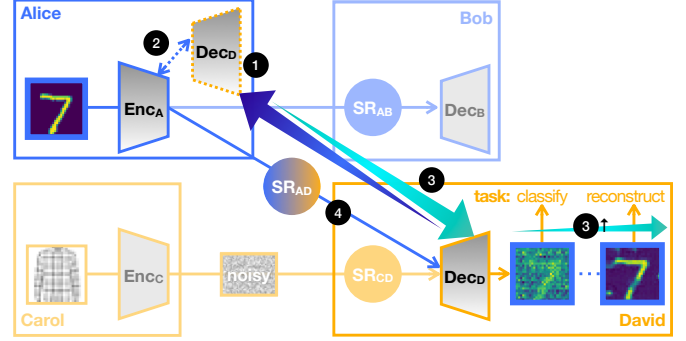


Fig. 1. A schematic illustration of split learning with layer freezing (SLF) with two DeepJSCC AEs: Alice-Bob AE and Carol-David AE trained under heterogeneous datasets (MNIST and Fashion-MNIST) and different levels of channel noise.

Following this principle, it is possible to train an NN to emulate (i) source coding and (ii) channel coding functionalities in classical communication systems [7]. In addition to (i) and (ii), an NN can simultaneously emulate two new SC functionalities: (iii) pre-processing for extracting semantics and (iv) post-processing to solve a downstream task. Deep joint source and channel coding (DeepJSCC) is one promising approach that can concurrently emulate (i)–(iv) by using the autoencoder (AE) NN architecture [2], [3] consisting of a set of encoder layers (ENC) and its paired decoder layers (DEC). The AE NN of DeepJSCC is trained for a given task, after which SRs are generated from raw data at an ENC and delivered to the DEC producing outputs for the given task.

B. Misalignment Multi-User Semantic Communication

While effective in various tasks ranging from image reconstruction [2] to visual question answering [8], due to its NN architecture, one fundamental limitation of DeepJSCC is its inherent bias towards *a)* source (training) data and *b)* ENC-DEC channel characteristics during training. To illustrate this by an example, as shown in Fig. 1, consider two DeepJSCC AEs, namely the AE ENC₁-DEC₁ of Alice and Bob, and the other AE ENC₂-DEC₂ of Carol and David, which were trained under different data source and/or channel environments. After training, Alice and Bob communicate their intended semantics, and so do Carol and Bob. However, between Alice and David (or equivalently Carol and Bob), the SRs generated by Alice may not always be interpreted as intended at David due to the absence of joint training for the cross-pair, specifically ENC₁-DEC₂. This *semantics misalignment problem* is particularly critical in mobile scenarios whereby any newly encountered transceivers are unlikely to be interoperable, restricting the scalability of multi-user SC.

C. Aligning Semantics via Split Learning with Layer Freezing

In this article, we focus on the aforementioned semantics misalignment problem for multi-user SC, and aim to make SC robust against dissimilar source data and/or channels with low latency as well as low communication and computation costs. We tackle this problem by aligning the semantics between different DeepJSCC transceivers, inspired from split learning (SL) that trains multiple NNs while shuffling the split-segments of the NNs [9]. To this end, we propose a novel DeepJSCC fine-tuning method, coined *SL with layer freezing (SLF)*. As depicted in Fig. 1, with two DeepJSCC transceivers, the operations of SLF are summarized into the following steps.

- ➊ **Decoder Downloading:** Alice first downloads David's decoder DEC_2 through *background communication*, which is in contrast to exchanging SRs through *foreground communication*.
- ➋ **Local Fine-Tuning:** By connecting the downloaded decoder with its local encoder, Alice locally re-trains $\text{ENC}_1\text{-DEC}_2$ using its own source data and the Alice-David channel statistics that can be obtained during background communication under channel reciprocity.
- ➌ **Fine-Tuned Decoder Uploading:** After obtaining the fine-tuned pair $\text{ENC}'_1\text{-DEC}'_2$, Alice uploads the re-trained DEC'_2 back to David.
- ➍ **Aligned SR Transmission:** Finally, Alice transmits SRs generated from ENC'_1 , and David can decode it using its DEC'_2 .

During the fine-tuning process in ➋, Alice can partially fix the layers of DEC_2 , and re-train only the remainder. Fine-tuning computation cost commonly increases with the number of trainable layers. Moreover, only the fine-tuned layers need to be uploaded from Alice to David in the background communication. Therefore, while the DEC_2 downloading latency remains the same in ➊, the number of frozen layers decreases the fine-tuning computation latency in ➋ and the uploading latency in ➌, resulting in longer *recovery time*, defined as the end-to-end SR alignment latency during ➊ – ➍.

On the other hand, for an image reconstruction task, our experiments show that the number of frozen layers increases the reconstruction errors after ➍. Consequently, there is a trade-off between reconstruction errors and recovery time, which can be balanced for a given task. For instance, classification tasks may not require high-fidelity reconstruction, allowing Alice to freeze more layers.

D. Contributions

The major contributions of this work are summarized as follows.

- We propose SLF, an NN fine-tuning technique for aligning the semantics between two DeepJSCC transceivers trained under dissimilar source data and/or channels.
- Focusing on the impact of the number of frozen layers, we delve into recovery time and goals for two different tasks, i.e., mean squared error (MSE) for reconstruction and accuracy for classification, under different levels of source and channel dissimilarities.

- By simulations, we corroborate that SLF works successfully under various semantic misalignment scenarios. Furthermore, the trade-off between recovery time and task-specific operation in the simulations further emphasizes the importance of our proposed SLF.

II. SYSTEM DESCRIPTIONS

The network under study comprises different pairs of DeepJSCC transceivers TRX_i and TRX_j that are identically constructed on a vector-quantized variational AE (VQ-VAE) architecture [10] for a common task, while each transceiver is independently pre-trained under different source data and channel characteristics. VQ-VAE is a well-established NN architecture, and is capable of performing joint source and channel coding [11]. To make VQ-VAE generate task-specific SRs while improving architectural reusability for different tasks, we consider a tripartite VQ-VAE by adding a set of layers into the standard bipartite VQ-VAE for encoding and decoding, as detailed next.

Transceiver Structure. Each transceiver $\text{TRX}_i = [\theta_i, \phi_i, \gamma_i]$ with $i \in \{1, 2\}$ is an NN that sequentially processes the following three different functions: $\text{ENC}_i(\cdot)$ for source-channel encoding, $\text{DEC}_i(\cdot)$ for source-channel decoding, and $\text{Task}(\cdot)$ for task-specific operations, which are parameterized by three blocks of NN weights θ_i , ϕ_i , and γ_i , respectively. Each TRX_i includes a transmitter TX_i and its paired receiver RX_i .

SR Encoding. TX_i stores θ_i and source data samples \mathbf{x}_i in a local dataset \mathcal{X}_i . The encoding of \mathbf{x}_i through NN layers is described as a function $\text{ENC}_{ij}(\cdot)$ mapping \mathbf{x}_i into the SR \mathbf{z}_{ij} that is transmitted to RX_j , i.e.,

$$\mathbf{z}_{ij} = \text{ENC}_{ij}(\mathbf{x}_i), \quad (1)$$

where the first and second subscripts of \mathbf{z}_{ij} identify TX_i and RX_j , respectively. Note that $\text{ENC}_{ij}(\cdot)$ depends not only on TX_i but also on RX_j , since its encoder-decoder is concurrently trained. Following the standard VQ-VAE, within $\text{ENC}_{ij}(\cdot)$, \mathbf{x}_i is first mapped into a latent variable \mathbf{z}'_{ij} , followed by vector quantizing \mathbf{z}'_{ij} into an $\mathbf{z}_{ij} = \mathbf{c}_{k^*} \in \mathcal{C}_{ij}$, where $k^* := \arg \min_{\mathbf{c}_k \in \mathcal{C}_{ij}} \|\mathbf{z}'_{ij} - \mathbf{c}_k\|_2$ with a trainable codebook $\mathcal{C}_{ij} = \{\mathbf{c}_1, \mathbf{c}_2, \dots, \mathbf{c}_K\}$. Consequently, the transmitted SR \mathbf{z}_{ij} is composed of the elements in K codewords.

Channel Model. The transmitted SR \mathbf{z}_{ij} is distorted by a noisy channel between TX_i and RX_j , which is modeled using the K -ary discrete memoryless channel (DMC) [12]. For a given DMC crossover probability ε_{ij} , the received SR $\hat{\mathbf{z}}_{ij}$ is determined by the following transition probability:

$$\Pr(\hat{\mathbf{z}}_{ij} = \mathbf{c}_k | \mathbf{z}_{ij} = \mathbf{c}_{k^*}) = \begin{cases} 1 - \varepsilon_{ij}, & \text{if } k = k^* \\ \frac{\varepsilon_{ij}}{K-1}, & \text{otherwise.} \end{cases} \quad (2)$$

In other words, the received SR $\hat{\mathbf{z}}_{ij}$ is identical to the transmitted SR $\mathbf{z}_{ij} = \mathbf{c}_{k^*}$ with probability $1 - \varepsilon_{ij}$, and otherwise becomes one of other $K - 1$ codewords with equal probability. Here, the channel statistics can be characterized by ε_{ij} that increases with outage probability or equivalently decreases with the signal-to-noise ratio, as elaborated in [13].

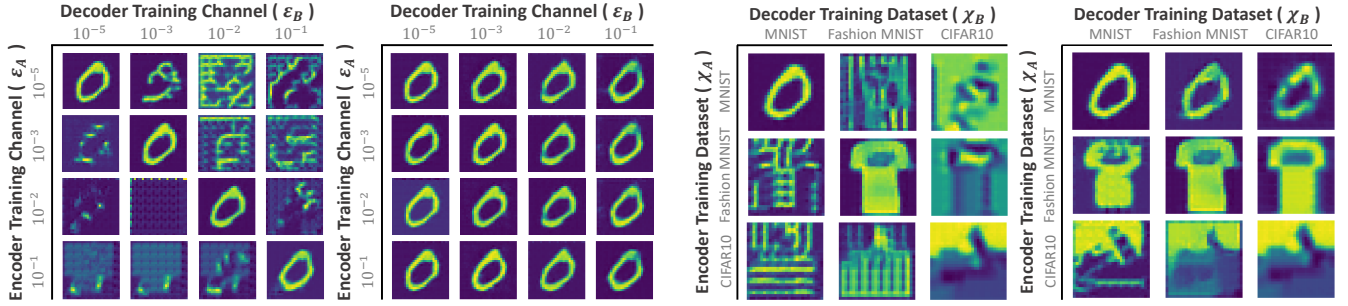


Fig. 2. Reconstructed images under different encoder-decoder training channels (1st and 2nd), and under different encoder-decoder training source data (3rd and 4th). Without SLF (1st and 3rd), off-diagonal images visualize the impact of semantics misalignment, which is fixed by SLF (2nd and 4th).

SR Decoding. At RX_j , it receives the distorted SR \hat{z}_{ij} , and yields the reconstructed sample \hat{x}_{ij} using the decoding function $DEC_{ij}(\cdot)$ as follows:

$$\hat{x}_{ij} = DEC_{ij}(\hat{z}_{ij}). \quad (3)$$

As a result, the end-to-end communication is summarized as $\mathbf{x}_i \xrightarrow{ENC_{ij}} \mathbf{z}_{ij} \xrightarrow{DMC} \hat{\mathbf{z}}_{ij} \xrightarrow{DEC_{ij}} \hat{\mathbf{x}}_{ij}$. The decoded sample \hat{x}_{ij} at RX_j can be different from the original sample \mathbf{x}_i at TX_i due not only to the channel noise but also to DEC_{ij} that was not jointly trained with $ENC_{i'j'}$, if $i \neq j'$. The latter warrants the need for addressing the semantics misalignment problem.

Task Effectiveness. The RX_j stores γ_j that utilizes \hat{x}_{ij} to carry out a task-specific decision-making $\text{Task}(\hat{x}_{ij})$. We consider two different tasks, source data sample reconstruction and the sample's label classification. For the reconstruction task, TRX_{ij} aims to minimize the MSE, $\mathbb{E}[\|\mathbf{x}_i - \hat{x}_{ij}\|^2]$, between the source sample \mathbf{x}_i and the decoded sample \hat{x}_{ij} . In this case, we have $\gamma_j = \emptyset$ and the structure of TRX_{ij} boils down to the standard bipartite VQ-VAE, i.e., $TRX_{ij} = [\theta_i, \phi_j]$, and $\text{Task}(\hat{x}_{ij}) = DEC_{ij}(\hat{z}_{ij}) = \hat{x}_{ij}$. On the other hand, for the classification task, we have $\gamma_j \neq \emptyset$, and TRX_{ij} aims to maximize the top-1 accuracy of the predicted label $\hat{y}_{ij} = \text{Task}(\hat{x}_{ij})$, for the given ground-truth label y_i associated with \mathbf{x}_i .

III. SPLIT LEARNING WITH LAYER FREEZING

A. Motivation – Challenges in Semantics Alignment

Suppose that there are two independently pre-trained Deep-JSCC transceivers TRX_i and TRX_j with $i \neq j$. The TX_i of TRX_i intends to communicate with RX_j of TRX_j . This misaligned SC is unlikely to be successful, in that TX_i 's θ_i and its original codebook \mathcal{C}_{ii} , as well as RX_j 's ϕ_j and γ_j are biased towards their separate pre-trained environments, in terms of its source data (i.e., \mathcal{X}_i and \mathcal{X}_j) as well as channel characteristics (i.e., ε_{ii} and ε_{jj}). Indeed, the off-diagonal examples in Figs. 2 show that misaligned SC fails in both the reconstruction task and classification task due to dissimilar channels and source data, respectively.

To make TX_i and RX_j interoperable, a naïve solution is to re-train a new transceiver $TRX_{ij} = [\theta_i, \phi_j, \gamma_j]$ through communication between TX_i and RX_j . However, this incurs non-negligible additional communication cost until re-training convergence. Furthermore, it may also violate data privacy, as it should share the local dataset \mathcal{X}_i of TX_i with RX_j at which the training loss is calculated by comparing RX_j 's output

with \mathcal{X}_i ; for instance, comparison with the original source sample \mathbf{x}_i for reconstruction or the ground-truth label y_i for classification.

Meanwhile, noticing that similar communication cost and data privacy issues have recently been tackled in the domain of distributed learning [1], one may attempt to tackle this semantics misalignment problem using federated learning (FL) [14], wherein clients train their local models in collaboration by averaging model parameters, without exchanging their private training datasets. Unfortunately, the semantics misalignment problem coincides with an extreme case of imbalanced data distributions across clients, also known as the non-independent and identically distributed (non-IID) data problem, under which the effectiveness of FL is significantly compromised [15]. In fact, our preliminary study in [16] demonstrates that FL only marginally improves convergence speed in re-training without any gain in accuracy, although it incurs significant communication cost due to exchanging model parameters per re-training iteration.

B. SLF for Aligning Semantics in Multi-User SC

Alternatively, to align semantics in multi-user SC, we propose a novel fine-tuning method, termed SLF. SLF leverages SL [17] to divide each transceiver into its encoder and decoder segments, followed by exchanging and fine-tuning different combinations of these segments. As visualized in Fig. 1, SLF operates in the following four steps.

- 1 TX_i downloads RX_j model parameters $[\phi_j, \gamma_j]$ while measuring ε_{ij} under uplink-downlink channel reciprocity.
- 2 TX_i partially freezes the downloaded model parameters, and locally fine-tunes a virtual transceiver $TRX_{ij} = [\theta_i, \text{Freeze}_\ell(\phi_j), \gamma_j]$ using \mathcal{X}_i under an applying measured crossover probability ε_{ij} , yielding a fine-tuned virtual transceiver $TRX'_{ij} = [\theta'_i, \phi'_j, \gamma_j]$.
- 3 TX_i uploads the fine-tuned unfrozen model parameters, i.e., non-zero elements of $[\phi'_j] - [\text{Freeze}_\ell(\phi_j)]$, to RX_j .
- 4 TX_i transmits the SR \mathbf{z}_{ij} encoded using θ'_i , and RX_j decodes the received \hat{z}_{ij} using $[\phi'_j, \gamma_j]$.

In 2, the function $\text{Freeze}_\ell(\cdot)$ freezes the ℓ -th layers of ϕ_j with $\ell \in \{0, 1, 2, \dots, L\}$ counting from the last layer. This counting order yields less performance degradation based on our experiments. The case $\ell = 0$ implies that ϕ_j is entirely re-trained. In this case we additionally apply parameter re-initialization before re-training, which improves the performance based on our experiments.

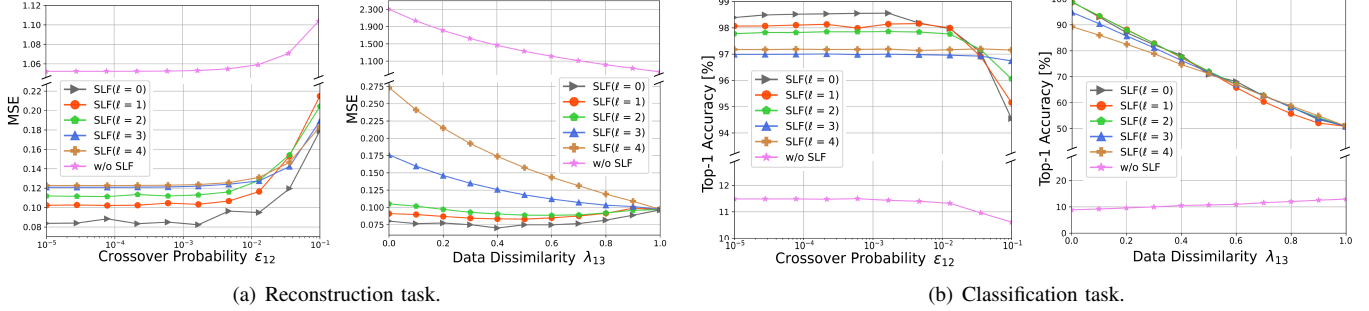


Fig. 3. Task-specific performance of SLF, i.e., MSE for reconstruction and top-1 accuracy for classification, under different DMC channel cross-over probability ε_{12} and source data dissimilarity λ_{13} .

The fine-tuning loss function of SLF follows from the standard VQ-VAE loss function \mathcal{L} given as follows [18]:

$$\mathcal{L} = \|\mathbf{x}_i - \hat{\mathbf{x}}_{ij}\|_2^2 + \|\hat{\mathbf{z}}_{ij} - sg[\mathbf{z}'_{ij}]\|_2^2 + \lambda_c \|sg[\hat{\mathbf{z}}_{ij}] - \mathbf{z}'_{ij}\|_2^2. \quad (4)$$

The terms λ_c is a constant hyper-parameter for the codebook commitment loss, and $sg[\cdot]$ is the stop-gradient operator for ensuring differentiability. Note that the first term in (4) coincides with the reconstruction task's MSE. For the classification task, the classifier γ_j is separately pre-trained and frozen, and no additional loss term is taken into account.

IV. NUMERICAL EVALUATION

To validate the effectiveness of SLF, we consider three transceivers TRX_i with $i \in \{1, 2, 3\}$, each of which consists of a pair of the jointly pre-trained transmitter TX_i and RX_i . The TX_i and RX_i components comprise 3 convolutional layers each, with Relu activation functions applied to all layers except the final one. The codebook for the VQ-VAE architecture was structured as a 16×16 embedding layer. As for the classifier responsible for the task-specific aspect, it consisted of a sequence of 2 consecutive convolutional layers followed by 2 linear layers. A common design pattern was employed by incorporating a maxpooling layer after each convolutional layer output. Hence, in the experimental setting, the freeze parameter ℓ can be configured within the range of 0 to 4, incorporating 3 convolution layers and 1 embedding layer.

The pre-training environment for TRX_i is characterized by the training datasets and the crossover probability ε_i of the DMCs, which are by default given as below.

- TRX_1 : MNIST dataset with $\varepsilon_1 = 10^{-5}$
- TRX_2 : MNIST dataset with $\varepsilon_2 = 10^{-1}$
- TRX_3 : CIFAR-10 dataset with $\varepsilon_3 = 10^{-5}$

We consider the semantics misaligned transceivers $[TX_1, RX_2]$ and $[TX_1, RX_3]$ to study the impacts of channel and source data dissimilarities, respectively.

During the pre-training phase (before SLF), each dataset is divided into training and test datasets in the ratio of 8 : 2. The batch size is 128, and the optimizer is Adam with the learning rate 10^{-3} . During the fine-tuning phase (in SLF) with $\ell \geq 1$, we follow the same setting, but the learning rate is reduced to 10^{-4} . If $\ell = 0$, the entire parameters are re-trained, in which we additionally apply re-initialization and use the original learning rate 10^{-3} .

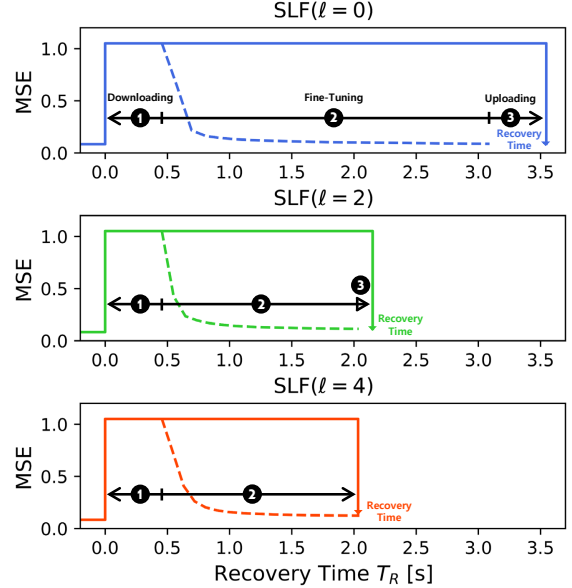


Fig. 4. Recovery time versus reconstruction MSE corresponding to parameter ℓ in SLF.

For a reconstruction task, TRX_{ij} has a bipartite structure: $TX_i = [\theta_i]$ and $RX_j = [\phi_j]$, where θ_i and ϕ_j follow the encoder and the decoder of a VQ-VAE NN. For a classification task, TRX_{ij} has a tripartite structure: $TX_i = [\theta_i]$ and $RX_j = [\phi_j, \gamma_j]$, where γ_j is a pre-trained classifier NN. In the codebook \mathcal{C}_{ij} , the number K of codewords is set as 16, which corresponds to the output and input dimensions of θ_i and ϕ_j , respectively.

Impact of Channel Dissimilarity. With $[TX_1, RX_2]$, we assume that channel statistics, i.e., ε_{12} , are known at TX_1 . Fig. 3 shows that SLF reduces the baseline MSE from a minimum of 84.6% to 92.1%. For classification, we increased the Top-1 accuracy by at least 67.1% and up to 70.9%. From the results showing the performance of various cases of ε_{12} and the freeze parameter ℓ for TX_1 and RX_2 , we can observe the following. The closer the environment RX_2 was trained in and the new environment TRX_{12} is facing, the more effectively the freeze parameter ℓ works. This means that we can further increase communication efficiency depending on the CSC problem, which we explain in more detail later when discussing latency.

Impact of Source Data Dissimilarity. The right side of each subfigure in Fig. 3 shows the SLF results according to the CSC problems caused by the difference in the trained data source environment. For a meaningful analysis according to

TABLE I
COMMUNICATION AND COMPUTATION COSTS OF SLF WITH RESPECT TO
THE NUMBER ℓ OF FROZEN LAYERS.

	$\ell = 0$	$\ell = 1$	$\ell = 2$	$\ell = 3$	$\ell = 4$
DL Payload Size [kBytes]	114	114	114	114	114
DL Latency [s] ①	0.456	0.456	0.456	0.456	0.456
Fine-Tuning Comput. [TFLOPS]	79.02	64.28	48.19	50.63	47.32
Fine-Tuning Latency [s] for Reconstruction ②	2.63	2.14	1.60	1.68	1.57
Fine-Tuning Comput. [TFLOPS]	75.43	67.49	39.69	37.31	34.17
Fine-Tuning Latency [s] for Classification ②	2.51	2.24	1.32	1.24	1.13
UL Payload Size [kBytes]	114	76	22	2	0
UL Latency [s] ③	0.456	0.304	0.088	0.008	0
Recovery Time [s] ① + ② + ③	3.542	2.900	2.144	2.144	2.026
Reconstruction MSE	0.087	0.103	0.113	0.121	0.123
Recovery Time [s] ① + ②' + ③	3.422	3.000	1.864	1.704	1.586
Classification Accuracy [%]	98.55	98.04	97.83	97.01	96.90

the data distribution, we assume that the dataset \mathcal{X}_1' sent by TX₁ follows the below formula.

$$\mathcal{X}_1' = (1 - \lambda_{13})\mathcal{X}_1 + \lambda_{13}\mathcal{X}_3, \quad (5)$$

where λ_{13} is defined as data dissimilarity. In this simulation, we use \mathcal{X}_1 as the MNIST dataset and \mathcal{X}_3 as the CIFAR10 dataset. To construct a classifier for the same comparison, we used the classifier γ_3 , which was trained on both MNIST and CIFAR10 datasets.

The results show when the dataset \mathcal{X}_1' has low data dissimilarity with \mathcal{X}_3 , RX₃ has trained, adjusting the freeze parameter ℓ according to the trade-off is abled. When $\lambda_{13} = 0$, the difference in SLF results based on the freeze parameter ℓ is 8.4% in the reconstruction task and 91.8% in the classification task. As the data dissimilarity becomes larger, the difference by the freeze parameter ℓ becomes smaller and finally converges to the same.

Recovery Time. We define recovery time as T_R which takes to resolve a CSC problem, details as from the time taken from a point CSC problem occurred to RX_j received the ϕ_j' from TX_i completely. T_R varies depending on the uplink (UL) and downlink (DL) channel capacity between the TX_i and RX_j, and the computing power of the TX_j. We set those values to 2Mbps, 2Mbps, and 30TFLOPS, respectively. The simulation environment is when TX₁ and RX₂ apply SLF to resolve the CSC problem at $\varepsilon_{12} = 10^{-5}$. Tab. I shows the difference in recovery time according to RX₂'s task-specific γ_2 . SLF with freeze parameter $\ell = 4$ had the fastest T_R of 2.026s and 1.586, respectively. But the reconstruction MSE and accuracy were the worst. This trade-off shows the potential for the proposed SLF to be dynamically adapted based on recovery time and performance.

V. CONCLUSION

In this paper, we addressed the issue of semantic misalignment arising from the nature of NNs in DeepJSCC with AI transceiver. To solve this problem, we proposed Split Learning with layer Freezing (SLF) and analyzed various scenarios depending on the key parameter in the SLF operation. With this promising solution, our study highlights the significance of achieving interoperability when constructing a communication system using an AI transceiver in a multi-user communication environment.

REFERENCES

- [1] J. Park, S. Samarakoon, A. Elgabli, J. Kim, M. Bennis, S. Kim, and M. Debbah, "Communication-efficient and distributed learning over wireless networks: Principles and applications," *Proc. IEEE*, vol. 109, pp. 796–819, May 2021.
- [2] E. Boursoulatze, D. B. Kurka, and D. Gündüz, "Deep joint source-channel coding for wireless image transmission," *IEEE Trans. Cogn. Commun. Netw.*, vol. 5, no. 3, pp. 567–579, 2019.
- [3] Z. Qin, X. Tao, J. Lu, and G. Y. Li, "Semantic communications: Principles and challenges," *arXiv preprint arXiv:2201.01389*, 2021.
- [4] H. Seo, J. Park, M. Bennis, and M. Debbah, "Semantics-native communication via contextual reasoning," *IEEE Trans. Cogn. Commun. Netw.*, pp. 1–1, 2023.
- [5] C. E. Shannon and W. Weaver, *The Mathematical Theory of Communications*. University of Illinois Press, 1949.
- [6] K. Hornik, M. Stinchcombe, and H. White, "Multilayer feedforward networks are universal approximators," *Neural networks*, vol. 2, no. 5, pp. 359–366, 1989.
- [7] F. A. Aoudia and J. Hoydis, "End-to-end learning of communications systems without a channel model," in *Proc. Asilomar*, (Pacific Grove, CA, USA), 2018.
- [8] H. Xie, Z. Qin, and G. Y. Li, "Task-oriented multi-user semantic communications for vqa," *IEEE Wireless Commun. Lett.*, vol. 11, no. 3, pp. 553–557, 2021.
- [9] P. Vepakomma, O. Gupta, T. Swedish, and R. Raskar, "Split learning for health: Distributed deep learning without sharing raw patient data," *Arxiv preprint*, vol. abs/1812.00564, Dec. 2018.
- [10] A. Van Den Oord, O. Vinyals, *et al.*, "Neural discrete representation learning," *Adv. Neural Inf. Process. Syst.*, vol. 30, 2017.
- [11] T.-Y. Tung, D. B. Kurka, M. Jankowski, and D. Gündüz, "Deepjssc-q: Constellation constrained deep joint source-channel coding," *IEEE J. Sel. Areas Inf. Theory*, 2022.
- [12] T. M. Cover, *Elements of information theory*. John Wiley & Sons, 1999.
- [13] M. Nemati and J. Choi, "All-in-one: Vq-vae for end-to-end joint source-channel coding," 2022.
- [14] B. McMahan, E. Moore, D. Ramage, S. Hampson, and B. A. y Arcas, "Communication-efficient learning of deep networks from decentralized data," in *Artificial intelligence and statistics*, pp. 1273–1282, PMLR, 2017.
- [15] Y. Zhao, M. Li, L. Lai, N. Suda, D. Civin, and V. Chandra, "Federated learning with non-iid data," *arXiv preprint arXiv:1806.00582*, 2018.
- [16] C.-H. Park, J. Choi, J. Park, and S.-L. Kim, "Federated codebook for multi-user deep source coding," in *2022 13th ICTC*, pp. 994–996, IEEE, 2022.
- [17] P. Vepakomma, O. Gupta, T. Swedish, and R. Raskar, "Split learning for health: Distributed deep learning without sharing raw patient data," *arXiv preprint arXiv:1812.00564*, 2018.
- [18] A. Van Den Oord, O. Vinyals, *et al.*, "Neural discrete representation learning," *Adv. Neural Inf. Process. Syst.*, vol. 30, 2017.